

LETTER

How do genetic correlations affect species range shifts in a changing environment?

Anne Duputié,^{1,2} François Massol,^{2,3} Isabelle Chuine,¹ Mark Kirkpatrick² and Ophélie Ronce⁴

Abstract

Species may be able to respond to changing environments by a combination of adaptation and migration. We study how adaptation affects range shifts when it involves multiple quantitative traits evolving in response to local selection pressures and gene flow. All traits develop clines shifting in space, some of which may be in a direction opposite to univariate predictions, and the species tracks its environmental optimum with a constant lag. We provide analytical expressions for the local density and average trait values. A species can sustain faster environmental shifts, develop a wider range and greater local adaptation when spatial environmental variation is low (generating low migration load) and multitrait adaptive potential is high. These conditions are favoured when nonlinear (stabilising) selection is weak in the phenotypic direction of the change in optimum, and genetic variation is high in the phenotypic direction of the selection gradient.

Keywords

Adaptation, climate change, gene flow, genetic constraints, multivariate evolution, range shift, spatial heterogeneity.

Ecology Letters (2012) 15: 251–259

INTRODUCTION

Ongoing global change is strongly affecting biodiversity, with numerous species currently becoming extinct, shifting in range, and/or changing their phenotype. Global species extinctions linked to climate change have already been observed (e.g. Parmesan 2006), and many more are expected in the coming decades, even under the overoptimistic scenario of unlimited dispersal (Thomas *et al.* 2004). Extinction can be avoided or delayed either through distributional range displacement or through trait evolution. Polewards shifts in distributional ranges are observed in many species, due to local population extinctions at low latitudes and/or colonisation at high latitudes (reviewed in Parmesan 2006; Hill *et al.* 2011). Plastic responses (e.g. Parmesan & Yohe 2003; Chevin & Lande 2010; Chuine 2010) and/or genetic responses (e.g. Bradshaw & Holzapfel 2001; Umina *et al.* 2005) could enable species to sustain environmental changes although not necessarily displacing their ranges. There is substantial interest in identifying those factors preventing species from adapting to changing environments, and thus setting range limits (e.g. Gaston 2003; Sexton *et al.* 2009). An important determinant of species' ranges may in particular be the potential for genetic adaptation of key traits to environments that change in space and time (Hoffmann & Sgrò 2011).

Both genetic constraints (e.g. genetic correlations between selected traits) and gene flow from maladapted populations have been offered as forces potentially constraining species adaptation. A recent model explored how these forces interact and contribute to maladaptation in

spatially heterogeneous landscapes (Guillaume 2011). Yet, no model has investigated these joint contributions in the context of an environment that changes both in time and space, as is the case for climate change over spatial gradients, which we herein set out to investigate.

Early models set in homogeneous environments focused on how demographic and genetic constraints influenced the maximal sustainable rate of change (Lynch & Lande 1993; Bürger & Lynch 1995). These models were subsequently generalised, to account for the multivariate nature of selection (Gomulkiewicz & Houle 2009). Indeed, if genetic variation seems to be present in virtually all traits studied (Brakefield 2003; but see Hoffmann *et al.* 2003 for a counterexample), genetic constraints can limit variation for some combinations of traits, making some phenotypes inaccessible to selection (Blows & Hoffmann 2005; Kirkpatrick 2009; Walsh & Blows 2009). For example, Etersson & Shaw (2001) found negative genetic correlations between traits that were under positive correlational selective pressures in an annual plant, which were predicted to slow adaptation to climate warming, as compared to univariate predictions. A review of empirical studies, however, shows that genetic correlations seem to help adaptation almost as often as they delay it (Agrawal & Stinchcombe 2009).

Spatial heterogeneity may also constrain species ranges (García-Ramos & Kirkpatrick 1997; Kirkpatrick & Barton 1997) because it leads to heterogeneous population density across the range. This generates asymmetric gene flow from central, dense populations

¹Centre d'Écologie Fonctionnelle et Évolutive – UMR 5175, campus CNRS, 1919, route de Mende, 34293 Montpellier Cedex 5, France

²Section of Integrative Biology, University of Texas at Austin, Austin, TX 78712, USA

³CEMAGREF – UR HYAX, 3275, route de Cézanne – Le Tholonet, CS 40061, 13182 Aix-en-Provence Cedex 5, France

⁴Institut des Sciences de l'Évolution (UM2-CNRS), Université Montpellier 2, Montpellier, France

*Correspondence: E-mail: anne.duputie@ens-lyon.org

towards peripheral populations with lower density. Such genetic swamping of peripheral populations may in turn prevent adaptation at the edge of the distribution range, and stop the expansion of the species. Even though the demographic importance of this migration load is unknown in natural settings (Sexton *et al.* 2009), empirical studies show that high migration rates prevent local adaptation, at least along steep gradients (e.g. Bridle *et al.* 2009). Along a constant linear environmental gradient, a cline is predicted to develop in the trait. If the gradient is sufficiently steep, the species has a finite range, which becomes smaller as genetic variance gets lower and/or the environmental gradient steeper (Kirkpatrick & Barton 1997). When the phenotypic optimum also changes linearly in time, the trait is still predicted to form a linear cline. If the change in time is sufficiently slow such that the species does not go extinct, its spatial distribution shifts, tracking the location where fitness is maximal (Pease *et al.* 1989). These results are not qualitatively altered by density regulation (Polechová *et al.* 2009). All these models, however, consider the adaptation of a single trait to changing environments. Herein, we address whether and how multivariate genetic constraints alter these predictions.

Our aim herein is to investigate the joint effects of multivariate genetic constraints and gene swamping on the demography and adaptation of a species faced with shifting environmental gradients. Building on the model by Pease *et al.* (1989), we focus on the evolutionary and demographical effects of (1) the temporally and spatially varying adaptive landscape, (2) multivariate genetic constraints and (3) dispersal abilities. We derive simple analytic approximations for the dynamics of trait means, the species' growth rate, the relative width of its distributional range, and the geographical lag in time between the location where fitness is maximal and that where population density is maximal. We show that the species' persistence and geographical range are maximised when the spatial

selection gradient, the direction of weakest stabilising selection and the direction of strongest genetic variance are aligned in phenotypic space. Our model generalises previous theory about species range evolution to the case of multivariate selection, and thus offers new opportunities for empiricists to quantify the constraints limiting adaptive responses to climate change in spatial context.

THE MODEL

A species inhabits a continuous landscape that varies along a single spatial dimension x . Its fitness is determined by d traits. The phenotype of a given individual at spatial location x and time t is denoted by vector $\mathbf{z}(x, t)$, and the average trait value at location x and time t is $\bar{\mathbf{z}}(x, t)$. The genetic covariance matrix \mathbf{G} and phenotypic covariance matrix \mathbf{P} are both assumed constant in time and space. Phenotypes and breeding values are assumed to be multivariate normally distributed. The notation used in this article is summarised in Table 1.

Individual dispersal mimics an unbiased diffusive process with constant diffusion rate σ . In ecological terms, σ^2 is the mean squared dispersal distance per unit time. The optimal phenotype changes linearly in space and in time (e.g. due to shifting latitudinal gradients in temperature, precipitation, resource availability). The vector of the slopes of these spatial gradients is denoted \mathbf{b} , and shifts in time at speed v (e.g. due to climatic change). The units of measurement of trait, space and time are scaled so that the optimal phenotype is $\mathbf{0}$ at time $t = 0$ and spatial location $x = 0$. The optimal phenotype at location x and time t is thus $\mathbf{b}(x - vt)$.

The fitness (that is, the intrinsic rate of increase) for an optimal phenotype is r_0 , and fitness decreases quadratically as \mathbf{z} deviates from that optimum:

$$r(\mathbf{z}, x, t) = r_0 - \frac{1}{2} [\mathbf{z} - \mathbf{b}(x - vt)]^T \mathbf{W}^{-1} [\mathbf{z} - \mathbf{b}(x - vt)] \quad (1)$$

Table 1 Notations used in this article and their dimensions

Notation	Designation in the text	Dimension
x	Space	$[x]$
t	Time	$[t]$
v	Rightward speed of the gradient shift (negative values indicate leftwards shift). By convention, positive values are used in this article	$[x] [t]^{-1}$
$\bar{r}(x, t)$	Mean fitness	$[t]^{-1}$
r_0	Rate of increase of an optimally adapted phenotype	$[t]^{-1}$
$\bar{\mathbf{z}}(x, t)$	Mean trait value [1-trait equivalent: $\bar{z}(x, t)$]	$[z]$
$n(x, t)$	Population density	-
\mathbf{b}	Environmental gradient of optimal trait values (1-trait equivalent: b)	$[z] [x]^{-1}$
σ^2	Variance of dispersal rate	$[x]^2 [t]^{-1}$
\mathbf{P}	Phenotypic covariance matrix. Assumed proportional to \mathbf{G} in simulations (1-trait equivalent: V_p)	$[z]^2$
\mathbf{G}	Genetic variance matrix. 1-trait equivalent: V_G	$[z]^2$
	Can be decomposed in $\sum_{i=1}^d \lambda_{\mathbf{G}_i} \mathbf{e}_{\mathbf{G}_i}$, where $(\mathbf{e}_{\mathbf{G}_i})$ form an orthonormal basis of \mathbb{R}^d	
\mathbf{W}^{-1}	Inverse of selection variance matrix: matrix of selection coefficients (1-trait equivalent: $1/V_S$)	$[z]^{-2} [t]^{-1}$
	Can be decomposed in $\sum_{i=1}^d \lambda_{\mathbf{W}_i^{-1}} \mathbf{e}_{\mathbf{W}_i^{-1}}$, where $(\mathbf{e}_{\mathbf{W}_i^{-1}})$ form an orthonormal basis of \mathbb{R}^d	
$\boldsymbol{\beta}$	Selection gradient, $\boldsymbol{\beta} = \mathbf{W}^{-1}(\bar{\mathbf{z}} - \mathbf{b}(x - vt))$	$[z]^{-1} [t]^{-1}$
$\boldsymbol{\beta}_x$	Spatial selection gradient, $\boldsymbol{\beta}_x = \mathbf{W}^{-1} \mathbf{b}$	$[z]^{-1} [t]^{-1} [x]^{-1}$
ϕ	Multitrait adaptive potential $\phi = \boldsymbol{\beta}_x^T \mathbf{G} \boldsymbol{\beta}_x$ (1-trait equivalent: $\phi_1 = b^2 V_G / V_S^2$)	$[x]^{-2} [t]^{-2}$
ψ	Spatial fitness contrast $\psi = \mathbf{b}^T \mathbf{W}^{-1} \mathbf{b}$ (1-trait equivalent: $\psi_1 = b^2 / V_S$)	$[x]^{-2} [t]^{-1}$
V_n	Proxy for the squared relative width of the distributional range	$[x]^2$
ρ	Overall growth rate of the population	$[t]^{-1}$
v_c	Critical speed of change above which the population will go extinct ($\rho < 0$)	$[x] [t]^{-1}$
L_n	Geographical lag between the location where fitness is maximal ($x = vt$) and the mode of population density	$[x]$
\mathbf{s}	Slopes of realised trait means (1-trait equivalent: s)	$[z] [x]^{-1}$

\mathbf{W}^{-1} is the symmetric positive-definite matrix describing the stabilising selection gradients. $\mathbf{W}^{-1} = -\boldsymbol{\gamma}$ in the Lande–Arnold formulation (Lande & Arnold 1983; see also eqns (3) in Phillips & Arnold 1989; and (1a) in Stinchcombe *et al.* 2008). The diagonal elements of \mathbf{W} measure the intensity of stabilising selection on the variances of each trait, with large values corresponding to weak selection, whereas its off-diagonal elements measure correlational selection on pairs of traits, i.e. selection for optimal combinations of trait values. Large diagonal entries in \mathbf{W} therefore denote traits for which large variance does not incur large fitness costs.

The mean population fitness, \bar{r} , is found by integrating over the phenotypic distribution, which gives:

$$\bar{r}(\bar{\mathbf{z}}, x, t) = r_0 - \frac{1}{2} \text{Tr}(\mathbf{W}^{-1} \mathbf{P}) - \frac{1}{2} [\bar{\mathbf{z}} - \mathbf{b}(x - vt)]^T \mathbf{W}^{-1} [\bar{\mathbf{z}} - \mathbf{b}(x - vt)] \quad (2)$$

where $\text{Tr}()$ is the trace operator. $\text{Tr}(\mathbf{W}^{-1} \mathbf{P})/2$ represents the fitness load that results from variation of phenotypes around the mean. The last term in eqn (1) denotes the mean loss of fitness at location x and time t , due to maladaptation: at a given point in space and time, fitness will be lowered all the more as $\bar{\mathbf{z}}(x, t)$ differs from the local phenotypic optimum $\mathbf{b}(x - vt)$. Since this optimum varies in time, the fitness of a given mean phenotype will vary in time at any given location (Fig. 1c). The fitness function above (eqn 2) is the multivariate equivalent to those used in univariate models, except that density is unregulated (unlike in Kirkpatrick & Barton 1997; Polechová *et al.* 2009). The fitness formula in Pease *et al.* (1989) can be reformulated in a similar way, with an additional term linked to fitness loss due to bad habitat quality. Namely, our model is equivalent to that of Pease *et al.* (1989) with (in their notation) $\rho = 1$, $m = 0$; w_{22} and w_{11} tending to infinity but keeping $b = \rho \sqrt{w_{22}/w_{11}}$ and $V_S = w_{22}(1 - \rho^2)$ finite (supporting information). Although our analytical model assumes no density regulation, the effects of logistic density regulation are studied through simulations in the supporting information.

Following univariate models (Pease *et al.* 1989; Kirkpatrick & Barton 1997; Polechová *et al.* 2009), the dynamics of the population density $n(x, t)$ at point x and time t are then:

$$\frac{\partial n}{\partial t} = \frac{\sigma^2}{2} \frac{\partial^2 n}{\partial x^2} + \bar{r} n \quad (3)$$

The first term of the right-hand side of eqn (3) represents diffusion from high to low density regions; the second term results from the net growth of the local population, depending directly on the matching between mean and optimum phenotypes (eqn 2). The dynamics of the vector of trait means are (multivariate extension of Pease *et al.* 1989):

$$\frac{\partial \bar{\mathbf{z}}}{\partial t} = \frac{\sigma^2}{2} \frac{\partial^2 \bar{\mathbf{z}}}{\partial x^2} + \sigma^2 \frac{\partial \ln(n)}{\partial x} \frac{\partial \bar{\mathbf{z}}}{\partial x} + \mathbf{G} \boldsymbol{\beta} \quad (4)$$

where $\boldsymbol{\beta}$ is the selection gradient (that is, the vector of partial derivatives of \bar{r} with respect to $\bar{\mathbf{z}}$: $\boldsymbol{\beta} = \mathbf{W}^{-1} [\mathbf{b}(x - vt) - \bar{\mathbf{z}}(x, t)]$). The first term of the right-hand side of eqn (4) represents the homogeneous diffusion of individuals with different trait values along the spatial axis; the second term reflects asymmetrical gene flow, with regions of higher population density sending more migrants towards regions of lower density. The third term corresponds to the response to multivariate selection through genetic adaptation. In spatially homogeneous environments, only this latter term remains, and the traits evolve according to the multivariate breeder’s equation (Lande &

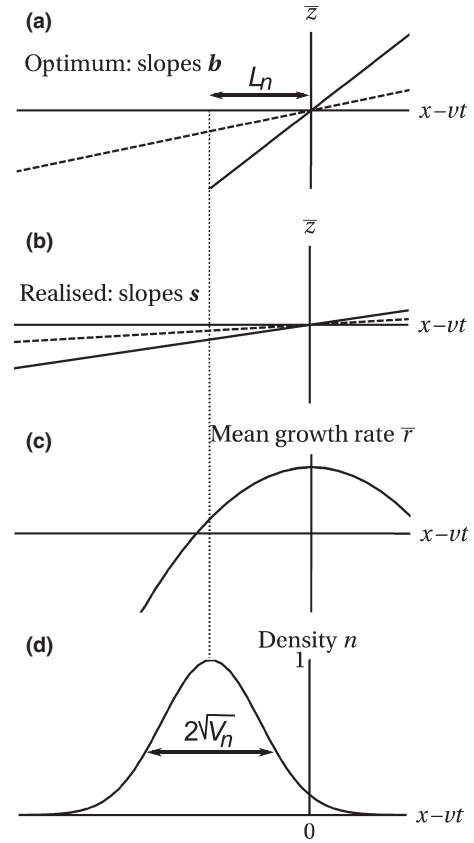


Figure 1 Optimal (a) and realised (b) phenotypes, mean population growth rate (c) and population density (d) across space and time $x - vt$. On panels a and b, traits 1 and 2 are shown as solid and dashed lines respectively. A displacement towards the left corresponds either to moving in space in a direction opposite to that of the shifting optima, or forwards in time. For example, individuals now located at $x = L_n + vt$ (vertical dotted line) have a low fitness, but maximal density, because they experienced higher fitness in the past (when they were located closer to the fitness optimum).

Arnold 1983). For a population whose mean trait value remains constant across space and time ($\bar{\mathbf{z}}(x, t) = \mathbf{0}$), $\mathbf{W}^{-1} \mathbf{b}$ measures how the selection gradient varies through space. Hereafter, $\mathbf{W}^{-1} \mathbf{b}$ will be referred to as ‘the spatial selection gradient’, and noted $\boldsymbol{\beta}_x$.

RESULTS

Population density and adaptation at steady state

The population reaches a dynamic equilibrium at which there is a Gaussian distribution of densities in space, and all traits show linear clines travelling at the same speed as the environmental shift (Fig. 1; supporting information). This bubble of density moves as a travelling wave described by:

$$n(x, t) = \exp\left(\rho t - \frac{(x - vt - L_n)^2}{2 V_n}\right) \quad (5)$$

While adaptation is described by:

$$\bar{\mathbf{z}}(x, t) = \mathbf{s}(x - vt) \quad (6)$$

Population density is Gaussian with constant relative width $2\sqrt{V_n}$ (Fig. 1d). Population density is maximal at a location where fitness is low, but used to be high. This location lags behind the location of

current maximal fitness by L_n (Fig. 1c,d). The total size of the population either grows or shrinks at an exponential rate given by ρ . Even though the relative width remains constant, if the population size grows ($\rho > 0$), the region hosting more than a given absolute threshold of individuals will expand, whereas it will shrink if the population shrinks ($\rho < 0$). Population size decreases towards the leading edge (right-hand side) of the distribution because of dispersal limitation, and towards the trailing edge (left-hand side) because of maladaptation (Fig. 1a,b). Numerical integration of the system formed by partial differential eqns (3 and 4) suggests that the following solution is unique (supporting information).

To find simple expressions for the lag L_n , the relative range size V_n , and the population growth rate ρ , we assume that $\|\mathbf{G}\mathbf{W}^{-1}\| \ll \sigma\sqrt{\mathbf{b}^T\mathbf{W}^{-1}\mathbf{b}}$. This situation is of interest because it results in a limited geographical range; otherwise the species is able to adapt everywhere (Kirkpatrick & Barton 1997; Polechová *et al.* 2009). Under this ‘strong migration load’ assumption, analytical approximations can be derived for the key variables ρ , V_n , L_n and \mathbf{s} (supporting information). All four of them depend on two key quantities (both strictly positive scalars, as long as $\mathbf{b} \neq \mathbf{0}$). The first is ϕ , which we call the ‘adaptive potential’. It measures the population’s potential to respond to selection, for a given deviation of local mean phenotype from optimal phenotype:

$$\phi = \beta_x^T \mathbf{G} \beta_x \tag{7}$$

The second key quantity is ψ , which we name the ‘spatial fitness contrast’. It measures the loss of fitness per space unit for any given phenotype:

$$\psi = \mathbf{b}^T \mathbf{W}^{-1} \mathbf{b} \tag{8}$$

The strong migration load approximation implies that $\phi \ll \sigma\psi^{3/2}$

At steady state, the equilibrium for the trait means consists of linear clines of slopes [eqn (9-13)] are given as Taylor series approximations to the first degree of $\phi/(\sigma\psi^{3/2})$:

$$\mathbf{s} \approx \frac{\mathbf{G}\beta_x}{\sigma\sqrt{\psi}} \tag{9}$$

(supporting information). With one trait, eqn (9) results in $s \approx V_G/(\sigma\sqrt{V_S})$. For most if not all traits, the slopes of the clines are generally much smaller in absolute value than are those of the optima \mathbf{b} . This leads to increasing maladaptation as $x - vt$ increases. Local adaptation is favoured when fitness varies smoothly across space (low ψ), but is countered by large dispersal because of the swamping effects of gene flow. Because the trait clines and the population density distribution move across space with the same speed v , the difference between optimal trait value and mean trait value, averaged over all populations across the range, stays constant in time.

An interesting implication of eqn (9) is that a ‘counter-gradient’ cline can develop whose slope is opposite in sign to the slope of its environmental gradient. This can occur because of indirect selection on negatively correlated traits: adaptation in one-trait causes another to evolve away from its optimum. Even in the absence of genetic correlations, however, a counter-gradient cline can develop if there is strong correlational selection, driving the spatial selection gradient in a direction of the multivariate space different to that of the optima \mathbf{b} . An example is shown in Fig. 2.

At steady state, the population growth rate is (supporting information):

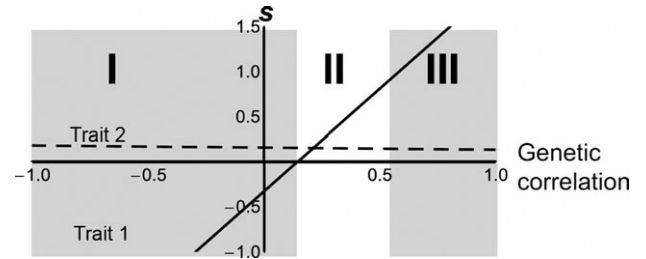


Figure 2 Realised trait slopes, as a function of genetic correlation. Fitness is determined by two traits whose optima vary linearly in space with slope 1. In this example trait 1 has more genetic variance and is under weaker stabilising selection than trait 2, and correlational selection is positive. Although trait 2 (dashed line) can never adapt completely, the slopes of the clines in trait 1 (solid line) can be either opposite to that of the optimum (domain I), lower but of the expected sign (domain II) or even higher (domain III). The width of each of these domains depends on correlational selection. Parameters used: $\mathbf{b}^T = (1, 1)$, elements of \mathbf{W} are $w_{11} = 1000$, $w_{22} = 10$ and $w_{12} = 20$; and elements of \mathbf{G} are $g_{11} = 1$, $g_{22} = 0.005$.

$$\rho \approx r_0 - \frac{1}{2} \left(\text{Tr}(\mathbf{W}^{-1} \mathbf{P}) + \sigma\sqrt{\psi} + \frac{v^2}{\sigma^2} \right) + \frac{\phi}{2\psi}, \tag{10}$$

Equation (10) shows that the population growth rate will be negative, and extinction will result, if the speed of the environmental change exceeds:

$$v_c \approx \sigma \sqrt{2r_0 - \text{Tr}(\mathbf{W}^{-1} \mathbf{P}) - \sigma\sqrt{\psi} + \frac{\phi}{\psi}} \tag{11}$$

Three types of fitness loads acting at the level of the whole range of the species can be identified from eqns (10 and 11) (Polechová *et al.* 2009): $\text{Tr}(\mathbf{W}^{-1} \mathbf{P})/2$ is the standing phenotypic load (due to variation around the optimal phenotype; univariate equivalent: $V_P/(2V_S)$), $\sigma\sqrt{\psi}/2$ is the dispersal load (due to individuals moving towards locations where they are maladapted; univariate equivalent: $\sigma b/(2\sqrt{V_S})$), and $v^2/(2\sigma^2)$ is the lag load (due to the temporal shift of the environment). The population growth rate and the sustainable rate of change increase as the fitness gain through adaptation $\phi/(2\psi)$ increases, i.e. when the potential for adaptation is large and the spatial fitness contrast is low. Equation (11) shows that dispersal σ will help the population escape the environmental change (σ term before the square root), but will decrease local adaptation ($\sigma\sqrt{\psi}$ term): the sustainable rate of change is maximised for intermediate dispersal.

The square of the relative range width is (supporting information):

$$V_n \approx \frac{1}{\sqrt{\psi}} \left(\sigma + \frac{\phi}{\psi^{3/2}} \right). \tag{12}$$

The distributional range is thus wider when the adaptive potential ϕ increases and when dispersal σ increases. This increase due to dispersal is lower than would be expected from diffusion only, due to genetic swamping (Kirkpatrick & Barton 1997). The range contracts as spatial fitness contrast ψ increases. When the gradient is gentle and genetic adaptation is large, V_n can grow towards infinity, leading to an unlimited range, as observed by Kirkpatrick & Barton (1997) and Polechová *et al.* (2009), and as is also true in Pease *et al.* (1989; supporting information).

The geographical lag between the locations of maximal fitness and of maximal population density can be approximated by:

$$L_n \approx -\frac{\nu}{\sigma\sqrt{\psi}} \left(1 + \frac{\phi}{\sigma\psi^{3/2}} \right), \tag{13}$$

Just like the relative width of the range, this lag widens when the gradient is shallow with high adaptive potential. In other words, the peak of population density occurs further from the location of optimal adaptation when the fitness cost resulting from being maladapted is low (low ψ), or can be countered by genetic adaptation (high ϕ). The lag is proportional to the speed of the shift of the gradient (ν), and decreases when dispersal (σ) is large, enabling the species to track its optimum more closely.

The accuracy of our approximations for \mathbf{s} , ρ , V_n and L_n was tested for 100 000 random combinations of parameters, half with $d = 2$ traits and half with $d = 5$ traits (supporting information). Approximations for ρ , L_n and V_n always lie within 5% of the exact values as long as $\varepsilon = \|\mathbf{G}\mathbf{W}^{-1}\| / (\sigma\sqrt{\psi}) < 10^{-1}$ (approximations for \mathbf{s} lie within 5% of the exact values when $\varepsilon < 10^{-2}$; supporting information). With $d = 5$ traits, the effective dimensionality of matrices \mathbf{G} and \mathbf{W}^{-1} was up to 4, with 95% of these matrices having fewer than two effective dimensions (*sensu* Kirkpatrick 2009; 95% of the 2-trait matrices had fewer than 1.7 effective dimensions). Regardless of the number of traits measured, \mathbf{G} -matrices for fitness-related traits seem to have fewer than two effective dimensions (Kirkpatrick 2009). Our simulated datasets therefore efficiently mimic real \mathbf{G} -matrices, and increasing the number of traits in our simulations would probably have little effect, even though the dimensionality of matrix \mathbf{W}^{-1} also has to be taken into account.

A geometric interpretation

Demographic parameters and adaptation are maximised when the potential to respond to selection ϕ is maximal, and when the spatial fitness contrast ψ is minimal. We can gain insight into how patterns of multivariate selection and genetic variation affect the evolution of the species' range, its growth rate and adaptation, by rewriting ϕ and ψ using the eigenvector decomposition of \mathbf{G} and \mathbf{W}^{-1} (as in e.g. Walsh

& Blows 2009). For a constant intensity of the spatial selection gradient $\|\boldsymbol{\beta}_x\|$, ϕ can be written as (supporting information):

$$\phi = \|\boldsymbol{\beta}_x\|^2 \sum_{i=1}^d \lambda_{\mathbf{G}_i} \cos^2(\mathbf{e}_{\mathbf{G}_i}, \boldsymbol{\beta}_x) \tag{14}$$

For a constant intensity of the change in optimum $\|\mathbf{b}\|$, ψ can be written as (supporting information):

$$\psi = \|\mathbf{b}\|^2 \sum_{i=1}^d \lambda_{\mathbf{W}_i^{-1}} \cos^2(\mathbf{e}_{\mathbf{W}_i^{-1}}, \mathbf{b}) \tag{15}$$

where $\lambda_{\mathbf{G}_i}$ and $\lambda_{\mathbf{W}_i^{-1}}$ are the i^{th} eigenvalues of \mathbf{G} and \mathbf{W}^{-1} ordered by decreasing values, $\mathbf{e}_{\mathbf{G}_i}$ and $\mathbf{e}_{\mathbf{W}_i^{-1}}$ are the corresponding eigenvectors, and $\cos(\mathbf{x}, \mathbf{y})$ is the cosine of the angle between vectors \mathbf{x} and \mathbf{y} .

Equation (14) and Fig. 3 show that, for a given strength of the selection gradient $\|\boldsymbol{\beta}_x\|$, the population's potential to adapt to changing conditions, measured by ϕ , is maximised when genetic variance is large (as indicated by large $\lambda_{\mathbf{G}_i}$) in the direction of the phenotypic space upon which selection is strongest ($\cos^2(\mathbf{e}_{\mathbf{G}_1}, \boldsymbol{\beta}_x) = 1$, i.e. $\mathbf{e}_{\mathbf{G}_1}$ parallel to the spatial selection gradient $\boldsymbol{\beta}_x$).

Equation (15) and Fig. 4 show that, for a given intensity of the change in optimum $\|\mathbf{b}\|$, the spatial fitness contrast ψ is minimised when selection is weak (weak stabilising selection, translating into low $\lambda_{\mathbf{W}_i^{-1}}$, and weak directional selection, translating into low $\|\mathbf{b}\|$), and when stabilising selection is weakest in the direction of the change in optimum \mathbf{b} .

Local adaptation increases, and all parameters of population density are maximised, when the adaptive potential ϕ is maximal, and when the spatial fitness contrast ψ is minimal. This occurs when selection is weak, genetic variance is large and occurs in the phenotypic direction of $\boldsymbol{\beta}_x$ (for a given $\|\boldsymbol{\beta}_x\|$) and when the change in optimum occurs in a phenotypic direction under weak stabilising selection (for a given $\|\mathbf{b}\|$). Figure 5 illustrates how the relative range width and the sustainable rate of change vary, depending on the relative orientations of the change in optimum and of the leading directions of genetic

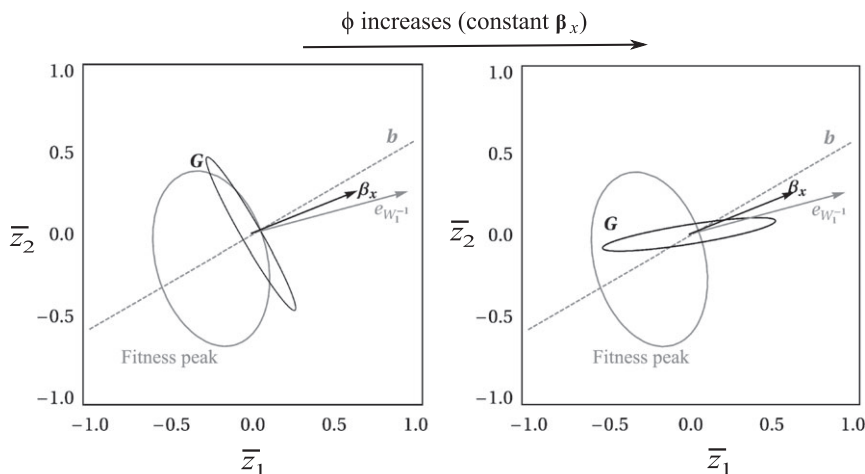


Figure 3 Variation of the potential for multivariate adaptation ϕ , as a function of the relative orientations of the spatial selection gradient and the leading direction of \mathbf{G} (black ellipses) in the phenotypic space (\bar{z}_1, \bar{z}_2). ϕ is maximal when most genetic variance (as indicated by the long axis of \mathbf{G}) is parallel to the spatial selection gradient $\boldsymbol{\beta}_x$, leading to maximised adaptation and enhanced demography. $\boldsymbol{\beta}_x$ follows from the environmental gradient (\mathbf{b} , dashed line) and maximal stabilising selection ($\mathbf{e}_{\mathbf{W}_i^{-1}}$, the direction of fastest fitness losses, as shown by the isofitness curve in grey). $\nu = 0.2$, $\sigma = 1$, $r_0 = 3$; $\mathbf{b} = \begin{pmatrix} 0.43 \\ 0.25 \end{pmatrix}$, $\mathbf{W}^{-1} = \begin{pmatrix} 1.10 & 0.56 \\ 0.56 & 0.50 \end{pmatrix}$; $\lambda_{\mathbf{G}_1} = 0.18$, $\lambda_{\mathbf{G}_2} = 0.02$ on both panels; covariances in \mathbf{G} are -0.76 on left panel and 0.38 on right panel, leading to $\phi = 0.0015$ and $\phi = 0.0107$ respectively.

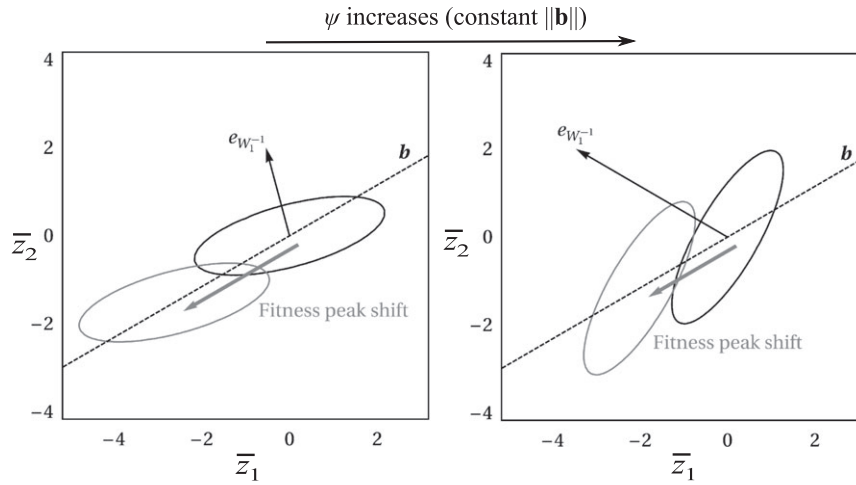


Figure 4 Variation of the spatial fitness contrast ψ as a function of the relative orientations of the change in optimum \mathbf{b} (dashed line) and the leading eigenvector of \mathbf{W}^{-1} (black) in the phenotypic space. A fitness contour is plotted for two different times on the same panel. Holding $\|\mathbf{b}\|$ constant, weaker fitness costs result when stabilising selection is weaker in the direction of \mathbf{b} (left vs. right panels), leading to higher adaptation and demographic variables on left panel than on right panel. Fitness contours are shown at $t = \infty/v$ (black) and $t = (x + L_n)/v$ (grey). $v = 1$, $\sigma = 1$, $r_0 = 3$, $\mathbf{b}^T = (0.43, 0.25)$, $\lambda_{\mathbf{W}^{-1}} = 1$, $\lambda_{\mathbf{W}^{-2}} = 0.1$ on both panels; covariances in \mathbf{W}^{-1} are 0.58 on left panel and -0.78 on right panel, leading to varying values of ψ (respectively 0.04 and 0.08).

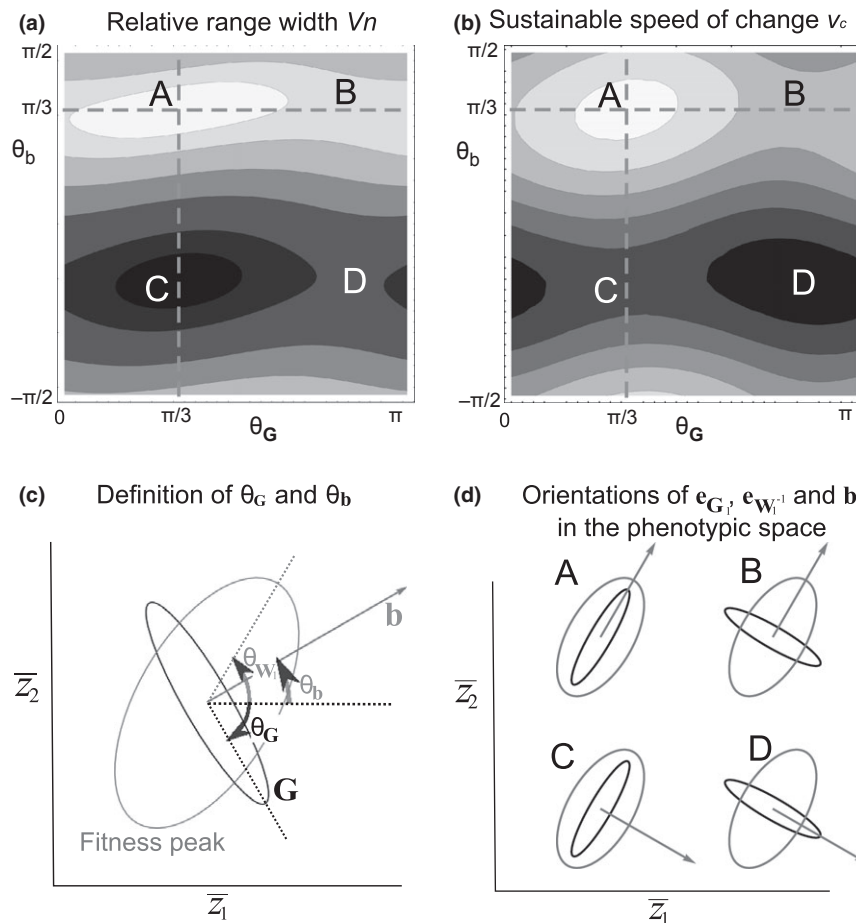


Figure 5 Demographic variables as a function of the orientations of \mathbf{b} (θ_b , ordinates) and of the leading eigenvector of \mathbf{G} (θ_G , abscissas) in the phenotypic space (panels a and b; these angles are defined on panel c). Lighter shades indicate higher values. The relative orientations of \mathbf{b} (grey), \mathbf{G} (black) and \mathbf{W}^{-1} (grey) are shown for four points on panel d (see main text; ψ is lowest in A and B and highest for C and D; ϕ is higher in A and D than in B and C). $\|\mathbf{b}\|$, $\lambda_{\mathbf{G}_1}$ and \mathbf{W}^{-1} are fixed, and weakest stabilising selection occurs in direction $\theta_{\mathbf{W}} = \pi/3$ (longest axis of the fitness contours on panels c and d). $\|\mathbf{b}\| = 1$; $\lambda_{\mathbf{G}_1} = 0.5$, $\lambda_{\mathbf{G}_2} = 0.1$, $r_0 = 0.1$, $\sigma = 1$, $v = 0.01$, $P = 4$ \mathbf{G} and the coefficients of \mathbf{W} are $w_{11} = 62.5$, $w_{22} = 87.5$, $w_{12} = 21.6$.

variance and stabilising selection. With the chosen settings (strong migration load, weak adaptation), the relative width of the range is much more sensitive to the spatial fitness contrast ψ than to the potential for multivariate adaptation ϕ . Widest ranges appear, as expected, when the change in optimum occurs in the direction upon weakest stabilising selection, and when genetic variance is maximally available in the direction of the spatial selection gradient (Fig. 5, point A). A similar pattern is observed for the sustainable speed of change (and for the growth rate), as long as the standing load is not too high. The sustainable speed of change is strongly affected by the migration load, and narrow ranges may not be indicative of populations at maximal risk from a given change (compare points C and D in Fig. 5).

DISCUSSION

Our model extends previous models developed in univariate settings (Pease *et al.* 1989; Polechová *et al.* 2009) and underlines the need to take multivariate interactions into account when assessing the capacity of a species to persist in a changing environment. Genetic correlations and the structure of selection (directional, stabilising and correlational) strongly affect the demography and the adaptive potential of species faced with environmental change. If they avoid extinction, populations will track their environmental optimum, all the more closely when dispersal is large compared to the speed of the shift, when the change in selection across space and time β_x occurs in a direction of the multivariate phenotypic space where genetic variance is widely available, and when stabilising selection pressures are weak in the multivariate direction of the change in optimum \mathbf{b} . These conditions also maximise the relative width of the range of the species and the lag it can sustain while tracking its optimal environment. If the standing phenotypic load is low, these conditions also maximise the species' growth rate.

How multivariate constraints modify univariate predictions

The addition of multivariate constraints in a spatial demo-genetic model of species adapting to environmental change generalises results of earlier univariate models. Qualitatively, our model recovers the predictions of univariate models with no or logistic regulation of population density (Pease *et al.* 1989; Kirkpatrick & Barton 1997; Polechová *et al.* 2009). Quantitatively, setting $d = 1$ trait, we recover all results found in the univariate no-regulation model of Pease *et al.* (1989) and, when also setting $\nu = 0$, in the univariate logistic regulation model of Kirkpatrick & Barton (1997); supporting information).

Multivariate constraints do not modify the prediction that the fastest changes can be sustained for intermediate rates of dispersal, which minimise maladaptation in peripheral populations, while allowing the species to track its fitness optimum across space. This has also been observed in univariate models taking genetic drift into account, because intermediate rates of migration minimise both the swamping effects of gene flow and the depletion in genetic variance due to drift in peripheral populations (Alleaume-Benharira *et al.* 2006).

In multivariate settings, however, wide ranges and efficient adaptation depend not only upon the magnitudes, but also on the relative orientations in the trait space, of genetic (co)variance, correlational and stabilising selection, and the change in optimum. Adaptation is promoted by the availability of genetic variance in the direction of the selection gradient (e.g. Lande & Arnold 1983; Blows

et al. 2004; Hellmann & Pineda-Krch 2007). When environmental gradients are steep, however, we show that it is of utmost importance for the persistence of the population that the change in optimum occurs in a direction that is under weak stabilising selection. We predict that the fastest changes can be sustained for intermediate rates of dispersal, which minimise maladaptation in peripheral populations, although allowing the species to track its fitness optimum across space. Our model emphasises the importance of environmental change occurring in a direction of the multivariate space upon which stabilising selection is weak. This is probably not always the case in nature. For example, phenological traits may be under strong stabilising selection, yet have to evolve fast in the face of climatic change. Plasticity may help species cope with changes, at least for some time (e.g. Charmantier *et al.* 2008).

For a species faced with a constant stress due to climate change (\mathbf{b} , \mathbf{W}^{-1} and hence ψ constant), persistence will be easier to achieve if fitness relies on few traits with large genetic variance, rather than on numerous traits that share the same total amount of variance, because the multivariate potential for adaptation ϕ is bounded above by $\|\beta_x\|^2 \lambda_{\max}$ (supporting information).

The existence of genetic correlations and/or correlational selection can constrain some traits to evolve in the opposite direction to that predicted from single trait studies (Lande 1979; Guillaume 2011). This may occur when both traits are selected in the same direction, but have negative genetic correlation. Whether or not the slope of one trait s_j will be of a sign opposite to that of the change in optimum for that trait (b_j) will depend upon the relative orientations of \mathbf{G} and β_x , and also of β_x and \mathbf{b} in the trait space. This will rely on both genetic correlations and correlational selection: in the absence of correlational selection, genetic covariances between traits may drive a few of them to develop counter-gradient clines; and in the absence of genetic correlations, correlational selection may drive β_x to point towards a different quadrant of the trait space than does vector \mathbf{b} , thus generating counter-gradient clines for some traits (Fig. 2). The clines observed in nature (or in a common garden) for a focal trait thus might not reflect the direction of the environmental gradient (e.g. Levins 1968). This can occur if an unmeasured trait is genetically correlated to the focal trait and is under stronger selection than the focal trait.

Robustness of model assumptions

Even though density is not regulated in our model, when there is a single trait and the gradient does not shift, our approximations for the relative range width and the slope of the trait mean are consistent with those found by Kirkpatrick & Barton (1997), in a model that includes logistic density regulation. This happens because range expansions rely on the shape of population density at the edges of the distribution, which is not modified by logistic density regulation. Numerical integration of eqns (3 and 4) with logistic density dependence showed critical rates of change that were very close to those found without density regulation (eqn11; supporting information). Our model thus seems robust to the addition of logistic density regulation, the only noticeable difference induced by logistic density regulation being the appearance of lags in trait means, in fast-changing environments (large ν). When density regulation has a different shape, however, the role of migration in limiting adaptation (Filin *et al.* 2008) and the speed of the travelling wave may be modified (Polechová *et al.* 2009).

To derive our approximations, we assumed that the migration load strongly exceeded the fitness gain through genetic adaptation

($\phi \ll \sigma \psi^{3/2}$). When the environmental gradient is shallow, stabilising selection is weak and/or genetic variance very large, this assumption is no longer true. Depending on the slopes of the environmental gradient, two regimes are possible in univariate models: limited adaptation with a limited range, and perfect adaptation with an unlimited range. When several traits are considered, this latter regime appears when $\sigma \psi^{3/2} < \phi$ (as in one-trait models; Kirkpatrick & Barton 1997; Polechová *et al.* 2009; Bridle *et al.* 2010). Our approximations do not hold in these situations. Situations where migration or environmental heterogeneity are null, and where adaptation is thus constant across space, are described by the models of Lynch & Lande (1993), Lande & Shannon (1996) and Gomulkiewicz & Houle (2009), which hold for panmictic populations inhabiting a spatially homogeneous landscape.

Extensions to this model

Our model makes the strong assumptions that selective pressures, environmental change and genetic variance are constant across space and time. These assumptions could be lifted through simulation studies, to better reflect the variations of selective pressures observed in natural settings. To accurately predict how a species can respond to environmental change, the next challenge is to quantify how genetic variances may evolve. Univariate models of adaptation along environmental gradients suggest that evolving genetic variances inflated by migration between divergent populations could readily lead to perfect adaptation (and unlimited ranges; Barton 2001; Guillaume & Whitlock 2007; Polechová *et al.* 2009). In the absence of strong genetic constraints, the **G** matrix is moreover predicted to evolve to align with the adaptive landscape (Blows *et al.* 2004; Jones *et al.* 2004; Guillaume & Whitlock 2007; Arnold *et al.* 2008), which may also facilitate adaptation in multivariate settings as considered in our model.

A further perspective is to consider that environmental gradients may not be linear, and most species certainly do not perceive their environments as continuous throughout their ranges. Another extension would be to allow the gradients to shift in time at different speeds (e.g. to account for different speeds of change in temperature and precipitation, ultimately leading to climates that have no current analogue). Indeed, if all gradients travel at the same speed, as presented above, this means that future environmental conditions are already represented at some point in space: in our model, environmental change cannot favour trait combinations that are not optimal currently at some point in space.

Making predictions in nature

Even though our model strongly simplifies natural processes, it can be used to predict whether or not a species is likely to sustain environmental change, provided that the prominent parameters can be estimated. The dispersal variance σ^2 (the variance of parent-offspring distance divided by generation time) can be estimated from genetic data (Broquet & Petit 2009). The speed of shift of the environmental gradient v can be estimated either from long-term measures of traits of given populations in the field, or from climatic projections. The shape of the fitness function can be estimated through regression of fitness over the traits (Lande & Arnold 1983; Schluter & Nychka 1994; Gimenez *et al.* 2009). Our model assumes that the variation of all traits relevant to fitness was captured. Vector **b** can be

estimated by comparing the fitness of a given population in different environments spanning the range of the species (by reciprocal transfer experiments, for example). Snapshot observations of natural clines, however, are not liable to yield accurate estimates of **b**, because clines may show slopes that are not representative of **b**, if genetic correlations and/or correlational selection exist (see above). Thus, comparing different phenotypes for each trait, in each environment (and ideally manipulating them) would lead to more accurate estimations of **b**, because the optimal phenotype could be derived readily for each trait in each environment. Alternatively, process-based models such as Phenofit (Chaine & Beaubien 2001) could be used to relate variation in traits (such as budburst date) to fitness.

If these estimates are roughly constant across locations, our model can be used to infer how likely it is that the species adapts and/or migrates to escape climate change. Numerous factors that are not considered in our model (notably habitat patchiness and biotic interactions; Case & Taper 2000; Gaston 2003; Goldberg & Lande 2006; Price & Kirkpatrick 2009) are likely to reduce the actual shift in range and the actual level of adaptation that the species might achieve. Nevertheless, our model can still be used to predict the optimistic expected outcome of environmental change on local populations, provided relevant traits are measured.

To predict whether or not species can track their optimum, we therefore need accurate estimations of the selective pressures stemming from environmental change, and quantification of the genetic and demographic constraints (Gomulkiewicz & Houle 2009). Importantly, given that genetic correlations are omnipresent in nature and that selection is intrinsically multivariate, studies aiming at predicting species response to environmental change should strive to include many traits to increase their predictive power.

ACKNOWLEDGEMENTS

We are grateful to Y. Dumont, J. Polechová, J. Roux, R. Shaw, D. Waxman for discussion and advice. R. Aguilée, A. Charmantier, L. M. Chevin, P. David, R. Holt, G. Martin and two anonymous referees provided useful comments on earlier versions of this manuscript. AD and FM were funded by European Commission's FP7 Marie Curie IOF grants (grants TRECC-2009-237228 to AD and DEFTER-PLANKTON-2009-236712 to FM); AD was also funded by a post-doctoral grant from the Axa Research Fund. This research was also supported by NSF grant DEB-0819901 to MK and by the French Agence Nationale de la Recherche grant EVORANGE (ANR-09-PEXT-01102) to OR, IC and AD. This is ISEM contribution 2011-228.

AUTHORSHIP

OR, IC and MK conceived the model; AD and FM designed and analysed the model; AD wrote the first draft of the manuscript and all authors contributed to subsequent revisions.

REFERENCES

- Agrawal, A.F. & Stinchcombe, J.R. (2009). How much do genetic covariances alter the rate of adaptation? *Proc. R. Soc. London Ser. B*, 276, 1183–1191.
- Allaume-Benharira, M., Pen, I.R. & Ronce, O. (2006). Geographical patterns of adaptation within a species' range: interactions between drift and gene flow. *J. Evol. Biol.*, 19, 203–215.

- Arnold, S.J., Bürger, R., Hohenlohe, P.A., Ajie, B.C. & Jones, A.G. (2008). Understanding the evolution and stability of the G-matrix. *Evolution*, 62, 2451–2461.
- Barton, N.H. (2001). Adaptation at the edge of a species' range. In: *Integrating Ecology and Evolution in a Spatial Context* (eds Silvertown, J. & Antonovics, J.). Cambridge University Press, Cambridge, UK, pp. 365–392.
- Blows, M.W. & Hoffmann, A.A. (2005). A reassessment of genetic limits to evolutionary change. *Ecology*, 86, 1371–1384.
- Blows, M.W., Chenoweth, S.F. & Hine, E. (2004). Orientation of the genetic variance-covariance matrix and the fitness surface for multiple male sexually selected traits. *Am. Nat.*, 163, 329–340.
- Bradshaw, W.E. & Holzapfel, C.M. (2001). Genetic shift in photoperiodic response correlated with global warming. *Proc. Natl Acad. Sci. USA*, 98, 14509–14511.
- Brakefield, P.M. (2003). Artificial selection and the development of ecologically relevant phenotypes. *Ecology*, 84, 1661–1671.
- Bridle, J.R., Gavaz, S. & Kennington, W.J. (2009). Testing limits to adaptation along altitudinal gradients in rainforest *Drosophila*. *Proc. R. Soc. London Ser. B*, 276, 1507–1515.
- Bridle, J.R., Polechová, J., Kawata, M. & Butlin, R.K. (2010). Why is adaptation prevented at ecological margins? New insights from individual-based simulations. *Ecol. Lett.*, 13, 485–494.
- Broquet, T. & Petit, E.J. (2009). Molecular estimation of dispersal for ecology and population genetics. *Ann. Rev. Ecol. Evol. Syst.*, 40, 193–216.
- Bürger, R. & Lynch, M. (1995). Evolution and extinction in a changing environment: a quantitative genetic analysis. *Evolution*, 49, 151–163.
- Case, T.J. & Taper, M.L. (2000). Interspecific competition, environmental gradients, gene flow, and the coevolution of species' borders. *Am. Nat.*, 155, 583–605.
- Charmantier, A., McCleery, R.H., Cole, L.R., Perrins, C., Kruuk, L.E.B. & Sheldon, B.C. (2008). Adaptive phenotypic plasticity in response to climate change in a wild bird population. *Science*, 320, 800–803.
- Chevin, L.-M. & Lande, R. (2010). When do adaptive plasticity and genetic evolution prevent extinction of a density-regulated population? *Evolution*, 64, 1143–1150.
- Chaine, I. (2010). Why does phenology drive species distribution? *Philos. Trans. R. Soc. London B*, 365, 3149–3160.
- Chaine, I. & Beaubien, E.G. (2001). Phenology is a major determinant of tree species range. *Ecol. Lett.*, 4, 500–510.
- Etterson, J.R. & Shaw, R.G. (2001). Constraint to adaptive evolution in response to global warming. *Science*, 294, 151–154.
- Filin, I., Holt, R.D. & Barfield, M. (2008). The relation of density regulation to habitat specialization, evolution of a species' range, and the dynamics of biological invasions. *Am. Nat.*, 172, 233–247.
- García-Ramos, G. & Kirkpatrick, M. (1997). Genetic models of adaptation and gene flow in peripheral populations. *Evolution*, 51, 21–28.
- Gaston, K.J. (2003). *The Structure and Dynamics of Geographic Ranges*. Oxford University Press, Oxford, UK.
- Gimenez, O., Grégoire, A. & Lenormand, T. (2009). Estimating and visualizing fitness surfaces using mark-recapture data. *Evolution*, 63, 3097–3105.
- Goldberg, E.E. & Lande, R. (2006). Ecological and reproductive character displacement on an environmental gradient. *Evolution*, 60, 1344–1357.
- Gomulkiewicz, R. & Houle, D. (2009). Demographic and genetic constraints on evolution. *Am. Nat.*, 174, E218–E229.
- Guillaume, F. (2011). Migration-induced phenotypic divergence: the migration-selection balance of correlated traits. *Evolution*, 65, 1723–1738.
- Guillaume, F. & Whitlock, M.C. (2007). Effects of migration on the genetic covariance matrix. *Evolution*, 61, 2398–2409.
- Hellmann, J.J. & Pineda-Krch, M. (2007). Constraints and reinforcement on adaptation under climate change: selection of genetically correlated traits. *Biol. Conserv.*, 137, 599–609.
- Hill, J.K., Griffiths, H.M. & Thomas, C.D. (2011). Climate change and evolutionary adaptations at species' range margins. *Annu. Rev. Entomol.*, 56, 143–159.
- Hoffmann, A.A. & Sgrò, C.M. (2011). Climate change and evolutionary adaptation. *Nature*, 470, 479–485.
- Hoffmann, A.A., Hallas, R.J., Dean, J.A. & Schiffer, M. (2003). Low potential for climatic stress adaptation in a rainforest *Drosophila* species. *Science*, 301, 100–102.
- Jones, A.G., Arnold, S.J., Bürger, R. (2004). Evolution and stability of the G-matrix on a landscape with a moving optimum. *Evolution*, 58, 1639–1654.
- Kirkpatrick, M. (2009). Patterns of quantitative genetic variation in multiple dimensions. *Genetica*, 136, 271–284.
- Kirkpatrick, M. & Barton, N.H. (1997). Evolution of a species' range. *Am. Nat.*, 150, 1–23.
- Lande, R. (1979). Quantitative genetic analysis of multivariate evolution, applied to brain: body size allometry. *Evolution*, 33, 402–416.
- Lande, R. & Arnold, S.J. (1983). The measurement of selection on correlated characters. *Evolution*, 37, 1210–1226.
- Lande, R. & Shannon, S. (1996). The role of genetic variation in adaptation and population persistence in a changing environment. *Evolution*, 50, 434–437.
- Levins, R. (1968). *Evolution in Changing Environments – Some Theoretical Explorations*. Princeton University Press, Princeton, New Jersey, USA.
- Lynch, M. & Lande, R. (1993). Evolution and extinction in response to environmental change. In: *Biotic Interactions and Global Change* (eds Kareiva, P., Kingsolver, J. & Huey, R.). Sinauer Associates Sunderland, Massachusetts, pp. 234–250.
- Parmesan, C. (2006). Ecological and evolutionary responses to recent climate change. *Ann. Rev. Ecol. Evol. Syst.*, 37, 637–669.
- Parmesan, C. & Yohe, G. (2003). A globally coherent fingerprint of climate change impacts across natural systems. *Nature*, 421, 37–42.
- Pease, C.M., Lande, R. & Bull, J.J. (1989). A model of population growth, dispersal and evolution in a changing environment. *Ecology*, 70, 1657–1664.
- Phillips, P.C. & Arnold, S.J. (1989). Visualizing multivariate selection. *Evolution*, 43, 1209–1222.
- Polechová, J., Barton, N.H. & Marion, G. (2009). Species' range: adaptation in space and time. *Am. Nat.*, 174, E186–E204.
- Price, T.D. & Kirkpatrick, M. (2009). Evolutionarily stable range limits set by interspecific competition. *Proc. R. Soc. London Ser. B*, 276, 1429–1434.
- Schluter, D. & Nychka, D. (1994). Exploring fitness surfaces. *Am. Nat.*, 143, 597–616.
- Sexton, J.P., McIntyre, P.J., Angert, A.L. & Rice, K.J. (2009). Evolution and ecology of species range limits. *Ann. Rev. Ecol. Evol. Syst.*, 40, 415–436.
- Stinchcombe, J.R., Agrawal, A.F., Hohenlohe, P.A., Arnold, S.J. & Blows, M.W. (2008). Estimating nonlinear selection gradients using quadratic regression coefficients: double or nothing? *Evolution*, 62, 2435–2440.
- Thomas, C.D., Cameron, A., Green, R.E., Bakkenes, M., Beaumont, L.J., Collingham, Y.C. *et al.* (2004). Extinction risk from climate change. *Nature*, 427, 145–148.
- Umina, P.A., Weeks, A.R., Kearney, M.R., McKechnie, S.W. & Hoffmann, A.A. (2005). A rapid shift in a classic clinal pattern in *Drosophila* reflecting climate change. *Science*, 308, 691–693.
- Walsh, B. & Blows, M.W. (2009). Abundant genetic variation + strong selection = multivariate genetic constraints: a geometric view of adaptation. *Ann. Rev. Ecol. Evol. Syst.*, 40, 41–59.

SUPPORTING INFORMATION

Additional Supporting Information may be downloaded via the online version of this article at Wiley Online Library (www.ecologyletters.com).

As a service to our authors and readers, this journal provides supporting information supplied by the authors. Such materials are peer-reviewed and may be re-organised for online delivery, but are not copy edited or typeset. Technical support issues arising from supporting information (other than missing files) should be addressed to the authors.

Editor, Lauren Buckley

Manuscript received 1 August 2011

First decision made 10 September 2011

Second decision made 22 November 2011

Manuscript accepted 13 December 2011